2024 European Conference on Computing in Construction
Chania, Crete, Greece
July 14-17, 2024

AN INTEROPERABILITY APPROACH FOR SOLAR CADASTER AT HIGH LATITUDES

Martina Giorio[1], Mattia Manni[1], Gilles Desthieux [2], Nesrin Irmak Köker[1], and Gabriele Lobaccaro[1]
[1]Department of Civil and Environmental Engineering, Faculty of Engineering, Norwegian University of Science and Technology (NTNU), Trondheim, Norway
[2]Haute école du paysage d'ingénierie et d'architecture de Genève, (HEPIA), University of Applied Sciences and Arts Western Switzerland (HES-SO), Geneva, Switzerland

Abstract

The climate change represents an opportunity to revolutionize the urban planning paradigms, turning the role of the cities from massive producers of carbon emissions and pollution into a more sustainable built environment through the exploitation of renewable energy sources. In this transition solar energy plays a key role. In this regard, the novel contribution of this work is twofold: i) providing an interoperability approach for a preliminary version of the solar cadaster for the municipality of Trondheim (Norway), located at high latitude; ii) exploiting the use of the solar cadaster to identify the most usable rooftop areas for solar systems' installations and as supportive instrument for public and private stakeholders to facilitate decision-making for urban energy planning.

Introduction

The revolution of the urban planning paradigms emerges as one of the challenges posed by the climate change. Cities, recognized as significant contributors to carbon emissions and pollutants, should evolve into more sustainable environments. In the energy field, this leads to active engagement by policymakers in exploring the urban potential for energy generation from renewable energy sources (RES). Reducing dependency on fossil fuels by optimizing the utilization of RES enables municipalities to mitigate the carbon footprint associated with their energy consumption (Chatzigeorgiou & Martinopoulos, 2023). Advanced and innovative technology solutions for RES exploitation contribute to this aim. In that regard, comprehensive and interactive urban energy planning platforms can facilitate the implementation of similar strategies within the built environment (Desthieux & Thebault, 2024). In fact, such platforms are designed to empower private and public stakeholders with the necessary insights for informed and timely decision-making. Particularly, instruments for urban energy planning which focus on solar energy potential (i.e., solar cadasters) can boost the adoption of active solar systems, either applied or integrated into the building envelope (i.e., roofs and facades) (Manni et al., 2023). Solar cadasters facilitate users in quantifying the solar irradiation impinging on urban surfaces (i.e., roofs, facades, and ground), enabling them to identify the most suitable areas for the installation of solar systems. However, integrating such instruments into the territorial database requires addressing issues related to interoperability of software performing specific tasks such as geometry reconstruction, solar modelling, outcomes post-processing, and data visualization (Manni et al., 2023).

The hereby study investigates the preliminary application of the solar cadaster developed by Desthieux et al. (Desthieux et al., 2018) to high-latitude locations, with a focus on the municipality of Trondheim, Norway. The Web platform developed in Geneva *(https://apps.sitg-lab.ch/solaire/)* showcases the solar cadaster to a wide public audience and related energy and economic indicators by buildings. Although locations at latitude greater than 60°N have traditionally been assumed to receive low solar irradiation, recent studies have pointed out that these areas show only slight differences from Continental Europe in terms of annual solar energy potential (Formolli et al., 2021, 2023).

This study aims to investigate interoperability between software for handling CityGML files (i.e., open-source 3D city modeling format that enables the representation, storage, and exchange of virtual city model) and those for territorial data processing, such as ArcGIS Pro, for managing 2D/3D vector and raster data. By implementing a platform for urban solar energy planning in Trondheim municipality, this work emphasizes the significance of incorporating solar energy potential data into territorial regulatory instruments.

The literature mentions several examples of solar maps (Bieda & Cienciała, 2021; Fish & Calvert, 2016; Kanters et al., 2014). Some of them are also published on web platforms such as the Oslo Solkart *(https://od2.pbe.oslo.kommune.no/solkart/)* and the Norwegian Solkart *(https://solkart.no/search)*. These two examples represent the most recent web platforms, developed at high latitudes, in Norway. The reviews reveal the following gaps. For example, the solar cadasters implemented by Saretta et al. (Saretta et al., 2020) and Jurasz et al. (Jurasz et al., 2020) for the Swiss territory and Poland, respectively, are unable to visualize the usable area on roofs for PV installation. This consists of the portion of the roofs' areas more suitable for PV installations, excluding other service plants (e.g., chimney, storage/service equipment, swimming pool) and architectural elements (e.g., windows, overhanging parts) as well as poorly irradiated areas (i.e., shaded parts of the roof, unsuitable roofs' surfaces exposures and orientation). Current solar cadasters usually consider the entire roof area as equally

useful (i.e., having the same solar energy potential level). However, to increase the reliability of the estimations, it is necessary to distinguish between area of the roof and usable area, as in London (Steadman et al., 2020) and Geneva (Desthieux et al., 2018) solar cadasters. There are very few studies and platforms providing estimations of the usable area, and none of them is developed for high-latitude applications. By examining the diverse web platforms, different levels of detail can be identified concerning the visualization of solar energy potential on the roofs. Among those, the most common two levels of visualization (LOV) are bidimensional (2D) exploiting either a solid (LOV1) or a gradient pattern (LOV2). The LOV1, which is the most common, corresponds to the lowest level of detail, and it associates a unique solar potential value with each roof slope. Conversely, the LOV2 enables visualizing the spatial variation of the solar energy potential with a color gradient. The level of visualization of this pattern strongly depends on the accuracy of the geometrical model. Solar cadasters with such level of visualization can show shadow cast from surrounding buildings as well as architectural and service plants elements of the roof (Amaro Silva et al., 2022), picturing the usable areas for installation of active solar systems. The Web platform of the solar cadaster of Geneva offers the LOV2 of visualization detail (Desthieux & Thebault, 2024).

Following the highlighted research gaps, the present study aims to investigate limitations and opportunities to improve the calculation and the visualization of the solar energy in the urban context, with a specific emphasis on high latitudes (Formolli et al., 2023). Identifying the available area for calculating the solar potential for a high latitude case study can be very valuable for advancing the research as there are still no studies with this level of detail.

Methods and materials

Case study selection

Three neighborhoods representative of low-, medium-, and high-density built areas in the city of Trondheim (N 63° 25' 41"), are selected as case studies to test the solar cadaster approach as introduced in Geneva. Their main characteristics are presented below in the Table 1 with the extension (m^2), the constructed volume (m^3), the built density, derived from the two previous values, and the normalized value of the density.

Table 1: List of the selected neighborhoods and information on their area and density

	Neighborhood area [m^2]	Buildings volume [m^3]	Density [m^2/m^3]	Normalized values
a	13662.12	5967.94	2.29	0.19
b	31098.13	4361.58	7.13	0.60
c	17665.09	2170.61	8.14	0.68

Besides the density, these neighborhoods differ in terms of their morphological characteristics and functions (Figure 1). The neighborhood (a) consists of a residential area with mostly two-story single-family detached houses, each with its private garden (i.e., high inter-building distances). Neighborhood (b) is also residential, but its houses are larger and taller compared to those in neighborhood (a). Gardens and courtyards are characterized by limited dimensions, thus increasing the risk of mutual shading between adjacent buildings. Finally, the neighborhood (c) is part of the downtown, and its buildings show a compact layout with small inner courtyards. In this area, stores open onto the ground level, while residential apartments are situated on upper floors.

Figure 1: Selected neighborhood (source: Google Earth). a) Pappenheim (low density), b) Rosenborg (medium density), c) Sentrum (high density).

Workflow

The workflow for the preliminary application of the solar cadaster platform developed by Desthieux et al. (Desthieux et al., 2018), at high-latitude locations, is outlined in Figure 2.

The solar model, encoded in JAVA, serves as the simulation engine, and constitutes the core of the workflow. Running it requires meteorological and geometrical input data. The meteorological input data are retrieved through the Meteonorm software version 7.3 *(https://meteonorm.com/)* provides statistical weather data representative of the period from 1990 to 2010 for a given location. Hourly data are averaged by month to shorten the dataset from 8,760 to 288 values. The geometrical input data consist of (i) digital surface model (DSM) of the analyzed neighborhoods for shadow casting, and the calculation slope and aspect on the area, (ii) the Shapefile containing 2D representation of buildings that provide an identifier and geometric data for each building, and (iii) the 3D model of the neighborhoods in CityGML format generated through the automated reconstruction technique from Kong and Fan (Kong & Fan, 2024). These are processed in ArcGIS Pro environment. Once the preparation of the input file is finalized, the solar simulation engine is started. The solar model is based on algorithms encoded in JAVA for the calculation of hourly, monthly, and yearly solar irradiation impinging on the studied area. The results are stored in Tag Image File (.TIF) format and can be visualized in ArcGIS Pro, utilizing various color gradients to represent the corresponding solar energy potential.

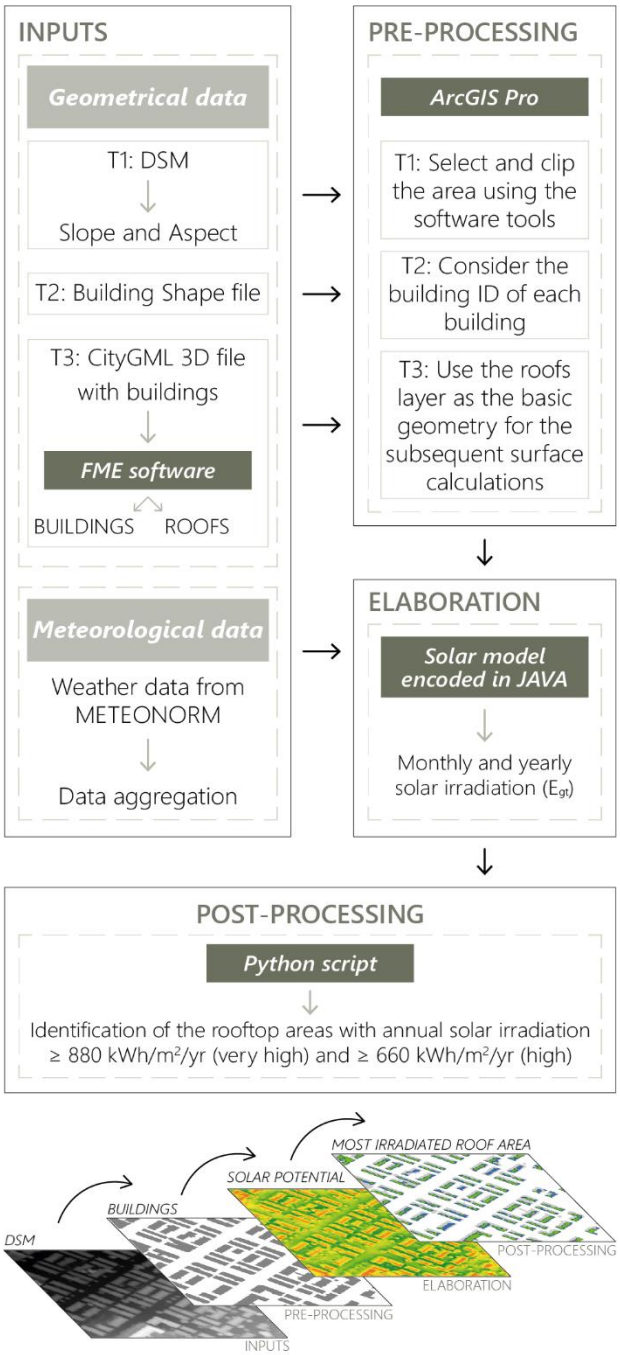

Figure 2: Workflow of the methodology developed in this study.

Following this, outputs from the solar model are post-processed to extract irradiation results on the roofs and identify the most suitable area on each roof for the installation of solar panels. Such an area consists of optimally exposed portions of the roof where there are no obstructions such as chimneys, roof windows, services, and machinery, hindering the installation of solar panels. Optimal exposition to solar irradiation is defined according to the threshold values identified for high latitudes in Lobaccaro et al. (Lobaccaro et al., 2019). Here in particular, the solar energy potential of any surface is labelled as 'very high' when the global tilted irradiation is greater than 880 kWh/m^2/yr; while it is classified as 'high' for global tilted irradiance amounts higher than 660 kWh/m^2/yr and lower than 880 kWh/m^2/yr. The range of low, medium, high, and very high solar irradiation is calculated based on the annual solar irradiation values for each surface, which are imported into 3D modelling software. The annual solar irradiation values are divided into five categories, for high latitudes: very low (0-220 kWh/m²/year), low (220-440 kWh/m²/year), medium (440-660 kWh/m²/year), high (660-880 kWh/m²/year), and very high (880-1.100 kWh/m²/year). These categories are determined based on the average values of solar irradiation in the middle point of each building's roof surface.

This part of the process (i.e., identification and classification of the most suitable area of the roof for solar panel installation), is conducting using a Python script. It represents a propaedeutic step for estimating the productivity of a potential PV system installed in the optimally irradiated portion of the roof.

The workflow is articulated and fragmented due to the utilization of different software and codifications, and it requires a high level of interoperability to integrate various type of information (i.e., meteorological, geometrical, and territorial vector and raster data) and data from different sources (e.g., HOYDEDATA.NO *https://hoydedata.no/LaserInnsyn2/*). This highlights the interdisciplinary and multi software domain of this research.

For this study, neighborhoods with an area ranging from 0.014 km^2 to 0.018 km^2 were selected to reduce the computational time for the solar analyses, compared to the whole city territory (340 km^2). Here the required time is represented by the time that the operator needs to manually perform the pre-processing tasks (T1-T2-T3). For each neighborhood, this can be estimated in 20 to 30 minutes. Considering the whole city of Trondheim, after the pre-processing time, needed for the selection of the different tiles, a total of around 50 hours are needed for the calculation of the solar potential results.

Pre-processing: preparation of input data for the solar modelling

Weather data are retrieved through Meteonorm software by choosing the nearest available weather station to the center of the city of Trondheim. The data are collected by the meteorological station at Værnes airport, located 35 km outside of the Trondheim municipality. The weather data file includes information about month of the year, hour of the day, global horizontal irradiation (Gh), diffuse horizontal irradiation (Dh), beam normal irradiation (Bn), and extraterrestrial irradiation (I_0). As mentioned in the workflow section, the solar analysis is conducted considering the average hourly values by month, rather than analyzing all days of the year (288 datapoints instead of 8,760). This permits to reduce both computational time and Central Processing Unit (CPU) requirements. The weather data is stored in a CVS format file. The other

input data for initializing the solar model is related to the neighborhood geometry.

DSM, Slope, and Aspect. The DSM data of the studied area is provided by The Norwegian Mapping Authority *HOYDEDATA.NO* in .TIF format with one-meter spatial resolution. The three case study neighborhoods are extracted from the Trondheim DSM file. Edge dimension of the three clipping masks range from 220 m to 420 m. To create the new DSM (i.e., the clipped DSM file of the investigated neighborhood), slope, and aspect files ArcGIS tools are used. The raster pre-processing outputs are stored in .TIF format: the DSM file has the pixel type of 32-bit float, and both slope and aspect files have a pixel type of 16-bit signed.

Building Shapefile. This is a two-dimensional file containing the building layouts of the city of Trondheim. It is retrieved from the national territorial database *GEONORGE* (FKB-Buildings Dataset, *https://kartkatalog.geonorge.no/metadata/fkb-bygning/8b4304ea-4fb0-479c-a24d-fa225e2c6e97*), and it contains information about the identifier for each building (i.e., LOKALID). The building shapefile of Trondheim is also clipped to isolate the three neighborhood case studies.

CityGML file. A Level of Detail 2 (LoD2) building model for the urban area of Trondheim is created through two main steps: (1) roof plane segmentation from building point clouds conducted by LIDAR airborne plane survey and (2) roof line topology-based building model creation in LoD2. A deep learning-based method (Zhang & Fan, 2022) was applied to automatically segment the building point clouds into roof planes. The obtained roof plane information served as the basis for reconstructing 3D roof structures and subsequently creating building models. In the second step, the LoD2 building models were created using roof line topologies (Kong & Fan, 2024). This process brought to the automatic reconstruction of building models in LoD2 for the Trondheim urban area. A file in CityGML format was exported from this model, containing three-dimensional information of the buildings. Using the FME software, it is divided into two separate outputs: one for buildings and another for roofs. In this study, only the second file (concerning the roofs) is considered. This was used as the geometric basis of the subsequent solar analyses.

Other studies developed in Europe (Adjiski et al., 2023) and in Asia (Dahal et al., 2021) use similar approaches for creating the geometrical models from LiDAR data as well as for identifying the best exposed portions of the roof through Geographic Information System (GIS) tools.

Elaboration: solar radiation modelling on the studied area

The JAVA-based solar model is initialized with the files described in the previous section. Additionally, information concerning the geolocation of the case studies (i.e., longitude, area of the studied zone, DSM resolution) is manually set, allowing for a more accurate estimation of the global tilted irradiation. It processes hourly solar radiation for each component: direct, diffuse and reflection, as well as shadow casting impacting direct (hourly-based) and diffuse, based on Sky View Factor (SVF), components. The solar modelling approach is introduced in Desthieux et al. (Desthieux et al., 2018).

Outcomes from the elaboration stage consist of 14 files in .TIF format, including a solar irradiation map for each month (12), the annual solar irradiation map (1), and the SVF map (1). These files are in a gradient form and permit to visualize the solar energy potential of roof and ground surfaces.

Post-processing: calculations and visualization in GIS

The annual solar irradiation map is post-processed to identify the most suitable areas which are available for PV installation. The thresholds defined in the workflow section are considered to extract the highly (global tilted irradiance within the range 660-880 kWh/m^2/yr) and very highly (global tilted irradiance within the range 660-880 kWh/m^2/yr) irradiated portions of the roofs. Therefore, the potential for energy generation through PV panels is investigated for these areas. (Lobaccaro et al., 2019)

For extracting the roof areas with high and very high solar potential, the annual solar irradiation map is multiplied by a clipping mask based on the roof footprints. The highly irradiated areas are highlighted by selecting raster pixels corresponding to irradiation amounts greater than 660 kWh/m^2/yr. Then, the same procedure is reiterated considering the threshold of 880 kWh/m^2/yr for very highly irradiated roofs.

Additionally, the raster pixels representing roof elements which can obstacle the installation of PV panels (i.e. ventilation systems, mechanical bodies, chimneys) are filtered out. A new polygon surface is created from these pixels and subtracted from the roof footprints, considering an inner buffer of 0.5 m, as the solar panels could not be installed in proximity of the building edges. The identification of the most adequate areas for PV installation is completed by removing from the analysis all the polygons with an area of less than 5 m^2. These surfaces are deemed too small for installation of PV systems. Finally, the solar PV production is calculated considering the available and optimally exposed areas of the roofs, as well as the characteristics of the installed PV panels. In this study, the monocrystalline PV is considered, with a peak power of 220 Wp/m^2 based on the most powerful models available on the market. Although flat roof configuration is not present in the investigated neighborhoods, it is worth mentioning that the potential PV energy production of flat roofs is quantified by assuming that PV panels are installed with a default inclination ranging from 10° to 15°. A transposition factor (FT) accounts for this aspect. Indeed, the use of flat roof configuration is becoming increasingly common at high latitudes, owing to the development of effective techniques for mitigating the accumulation of snow.

Results and Discussion

Solar irradiation analysis

Results about the estimated annual solar irradiation for the three case study neighborhoods resulting on the annual solar irradiation values range between 0 kWh/m^2/yr and 1,170 kWh/m^2/yr (Figure 3).

In neighborhood ‘a’ (low-density), most of the surfaces are optimally exposed to solar irradiation. In fact, the houses are small and far, while streets are wide, allowing for a better solar accessibility. In neighborhood ‘b’ (medium-density), the areas subject to high solar irradiation are fewer and limited to south-exposed roof slopes. In the neighborhood ‘c’ (high-density), the rooftop areas suitable for PV installation are minimal due to mutual shading among buildings.

The results of this approach demonstrate the importance of conducting detailed solar analyses within urban environments, utilizing interoperable software.

Determination of suitable areas for PV installation

Solar irradiation outputs are post-processed to exclude parts of the roof that are either unavailable or characterized by global tilted irradiance lower than 660 kWh/m^2/yr. These surfaces are shown in differentiating between highly and very highly irradiated surfaces (Figure 4) (see the Methods and Materials section for the applied thresholds). The numerical results concerning the surface area are reported in Table 2.

Table 2: Calculation of total roof areas and actual usable parts after the analysis

	Total roof area (m^2)	Available area with E_{gt} > 660 kWh/m^2/yr (m^2)	Available area with E_{gt} > 880 kWh/m^2/yr (m^2)
a	2069.45	1023.44	400.20
b	2546.77	1121.32	545.37
c	1666.46	688.67	114.01

Results highlight the differences that exist among the investigated neighborhoods in terms of solar accessibility and solar energy potential. When considering the area of highly irradiated surfaces, this ranges from 40% (neighborhood ‘c’) to 50% (neighborhood ‘a’) of the total neighborhood area in each case study. Conversely, the portions of roofs with a very high solar potential varies between 6% (neighborhood ‘c’) to 20% (neighborhood ‘b’) of the total neighborhood area (Table 3).

Table 3: Percentages of usable area after changing the minimum irradiance threshold

	% of usable area with E_{gt} > 660 kWh/m^2/yr	% of usable area with E_{gt} > 880 kWh/m^2/yr
a	49.45 %	19.34 %
b	44.03 %	21.41 %
c	41.33 %	6.64 %

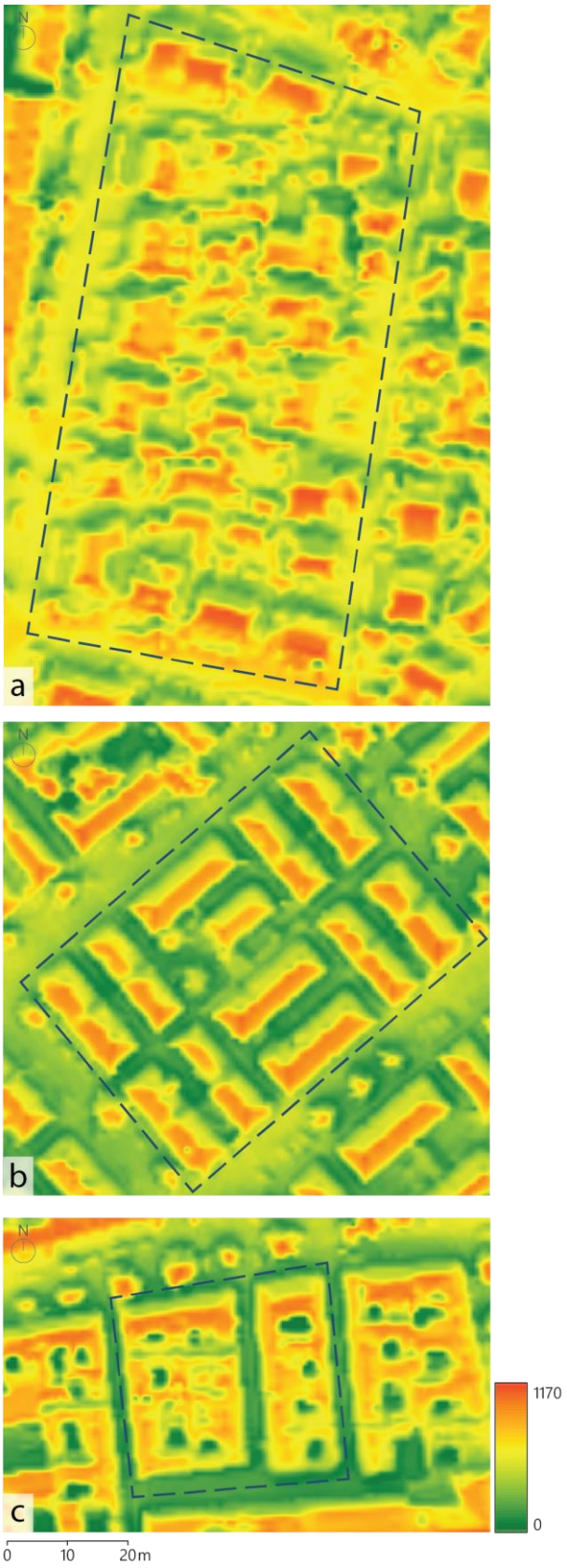

Figure 3: Annual solar irradiation (kWh/m^2/yr) calculated in the three neighborhoods.

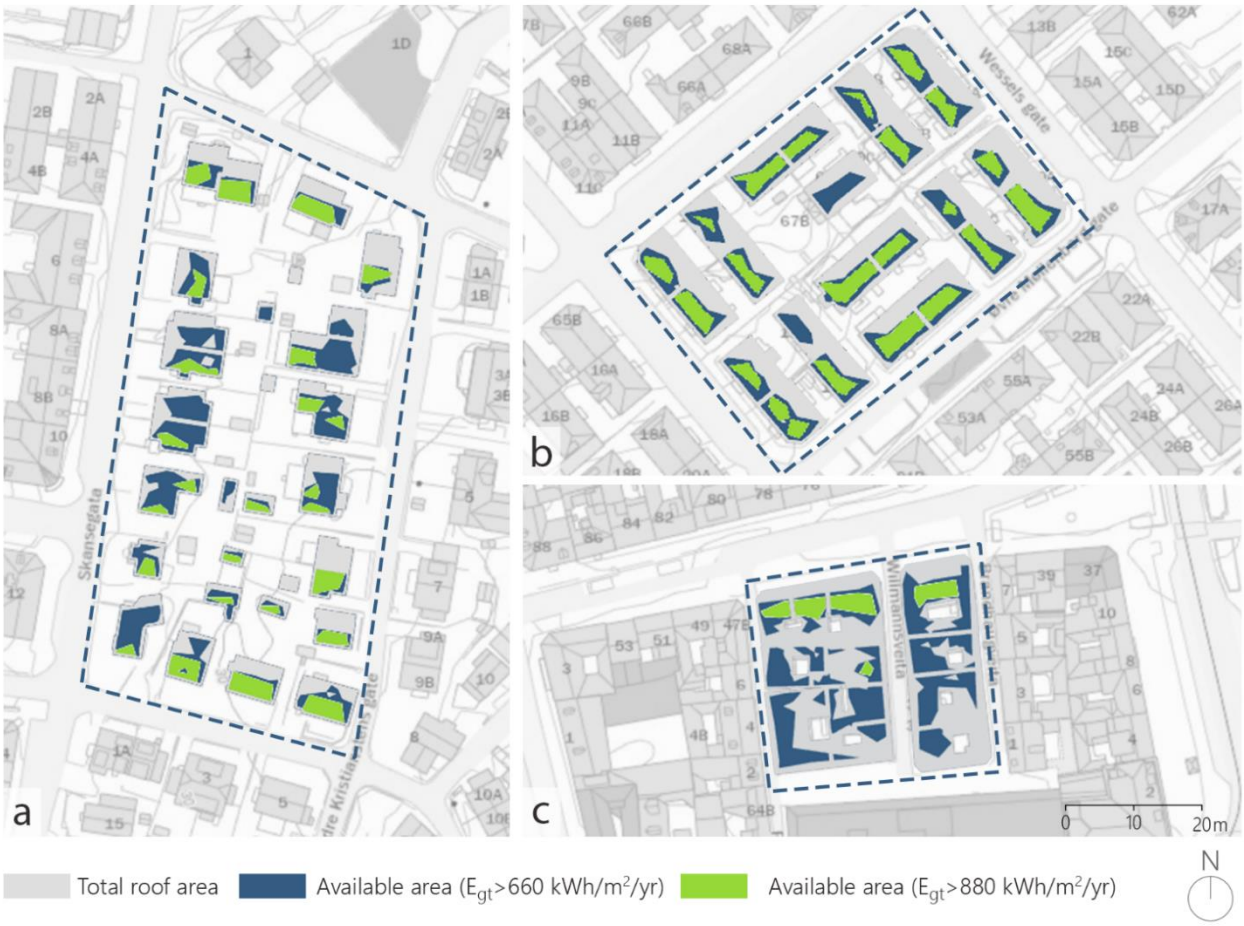

Figure 4: Available roof area resulted considering E_{gt} higher than 660 kWh/m2/yr and 880 kWh/m2/yr.

The limited number of neighborhood case studies (3) prevents conducting robust correlation analysis between neighborhood density and the total area of available surfaces for PV installation. Nonetheless, it is worth highlighting that, among the percentages reported in Table 3, the lowest value is always associated to the high-density neighborhood.

This is due to (i) the proximity of the buildings, which facilitates mutual shading, and (ii) the lower ratio of the roof area to the total area of the building's envelope, resulting in a greater presence of elements installed on a rooftop compared to neighborhoods 'a' and 'b'.

Comparison with existing solar modeling tools

ArcGIS geoprocessing tools such as the Raster Solar Radiation tool *(https://pro.arcgis.com/en/pro-app/latest/tool-reference/spatial-analyst/raster-solar-radiation.htm)* allow for conducting solar analyses with shorter computational time. However, they require the utilization of other models for calibration (Choi et al., 2019; Kausika & van Sark, 2021). Furthermore, those methods are characterized by a low level of users' customization (i.e., forced data inputs) of the simulation parameters, particularly, the temporal resolution that is fixed to one year. The use of more interoperable software permits to perform sub-yearly analysis, allowing the customization of input parameters such as weather data sources and time intervals.

Two online platforms for the visualization of the solar potential of roof surfaces are already available in Norway. These are characterized by different spatial scales: the Solkart spans across the whole country, while the Oslo Solkart covers the Oslo municipality. A visual comparison of the national Solkart and the solar cadaster approach applied in this study is shown in Figure 5.

There is a difference in the spatial resolution of the output data. The Solkart shows the solar potential of any roof slope as uniformly distributed, providing a single solar irradiance value for each surface. The Oslo Solkart has gradient values, but both existing Solkart neglect the identification of the rooftop areas suitable for PV installation considering the presence of obstructions or lower level of irradiation. The presented approach, on the other hand, provides a solar irradiance value for each pixel of the neighborhood's raster image, presenting a heterogenous spatial distribution of the solar irradiation on any rooftop slope. The calculation of the irradiation value on each part of the roof made it possible to identify the areas that are exposed to irradiation greater than 660 kWh/m^2/yr and 880 kWh/m^2/yr, highlighting the area available for new installations.

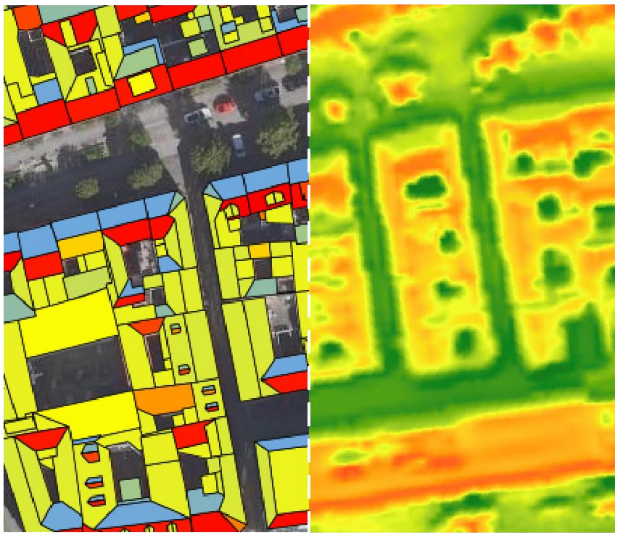

Figure 5: Visual comparison between the Solkart (left) and the solar cadaster approach from (Desthieux et al., 2018) *(right), applied to neighborhood 'b' (medium density).*

Finally, while the solar analysis performed with the Solkart does not account for the presence of trees, the method developer in the solar cadaster from (Desthieux et al., 2018) demonstrates the capability to process shadows casted from urban greenery included in the DSM.

Limitations of the study

This research study has three main limitations. Firstly, the weather data retrieved from Meteonorm v7.3 are collected by the meteorological station at Værnes airport, located 35 km outside of the Trondheim municipality. Indeed, this is the closest weather station to Trondheim which is available in Meteonorm database. Meteonorm was chosen over local weather stations to ensure a generic and easily replicable workflow for other case studies. Having more local data would allow for a more accurate analysis. Secondly, developing the process by implementing multiple software and tools allowed the results to be detailed, but at the same time having all the different working environments and code programming languages led to a fragmented process. The process is not automated, and the file recognition steps need to be filled in manually when switching from a software to another. Finally, only three case studies are considered for the calculation of the available roof area for PV installation. This limits the capability of identifying strong correlations between the model outputs and neighborhood density. Increasing the number of neighborhood case studies and expanding the analyses to the whole city of Trondheim can reinforce the conclusions drawn.

Processing the whole city of Trondheim will require to use the GPU machine installed at HEPIA (Stendardo et al., 2020), as for the solar cadaster in Geneva, which in particular allows to speed up the calculation of shadows implemented in the CUDA language.

Processing the solar analysis of a tile with a surface area of 9 km^2 takes approximately from one 1 to 1.5 hours. Therefore, analyzing the whole city of Trondheim, which has an area of 340 km^2, would take from 50 to 55 hours, which is acceptable for such an area. Computational time could be improved through parallelization.

Conclusions

The solar cadaster approach developed by Desthieux et al. (Desthieux et al., 2018) is applied to three neighborhoods in Trondheim (i.e., low-, medium-, and high-density neighborhoods). The proposed method is at the forefront of interoperability between software for managing urban geometry models and those for processing territorial data. The main findings of the study concern the identification of the best irradiated portion of the roofs suitable for installing PV systems. Results demonstrate the need for more refined analyses compared to existing online platform in Norway. Achieving this level of precision currently requires a combination of various software and types of information (i.e., meteorological, geometrical, and territorial vector and raster data). From the social perspective, the proposed solar cadaster approach aligns with the ongoing trend toward smart and sustainable cities. Informing citizens and municipalities about the solar potential of the building stock reflects a commitment to harnessing affordable and user-friendly technology for creating more efficient, sustainable, and livable built environments (Xue et al., 2021). Future advancements in this field may concern (i) enhancing the workflow through automation, parallelization, and reduction of the fragmentation to reduce the computational time especially for the whole city territory; (ii) exploiting the use of the local data and validating the results against real measurements; (iii) extending the analysis to the entire city territory of Trondheim; and (iv) creating an accessible online platform (i.e., solar cadaster) at the cityscape level to engage public and private stakeholders and the interaction with the individual users. Additionally, (v) extending the analysis to vertical surfaces (i.e., the facades) by including the optical properties of materials and the detection of architectural elements (i.e., windows, doors, balconies, overhanging parts) in the calculation will be important to increase the level of information on the most irradiated parts of the facades, especially at high latitudes where the vertical surfaces received the annual highest irradiance (Formolli et al., 2023). Therefore, it will be necessary to progress the research about material detection and image recognition techniques.

Acknowledgments

The authors gratefully acknowledge the support from the Norwegian Research Council (research project FRIPRO-FRINATEK no. 324243 HELIOS - eHancing optimal ExpLoitation of Solar energy in Nordic cities through the digitalization of built environment).

References

Adjiski, V., Kaplan, G., & Mijalkovski, S. (2023). Assessment of the solar energy potential of rooftops using LiDAR datasets and GIS based approach. *International Journal of Engineering and Geosciences*, *8*(2), 188–199. https://doi.org/10.26833/ijeg.1112274

Amaro Silva, R., Blanc, P., & Blanc OIE, P. (2022). Estimating Global Horizontal Irradiance at the Urban Level: A Sensitivity Analysis Using Different Digital Surface Models. *8th World Conference on Photovoltaic Energy Conversion*. https://www.researchgate.net/publication/363663602

Bieda, A., & Cienciała, A. (2021). Towards a Renewable Energy Source Cadastre - A Review of Examples from around the World. *Energies*, *14(23):8095*. https://doi.org/https://doi.org/10.3390/en14238095

Chatzigeorgiou, E., & Martinopoulos, G. (2023). Solar cadastre for assessment of near-zero energy districts. *IOP Conference Series: Earth and Environmental Science*, *1196*(1). https://doi.org/10.1088/1755-1315/1196/1/012003

Choi, Y., Suh, J., & Kim, S. M. (2019). GIS-based solar radiation mapping, site evaluation, and potential assessment: A review. *Applied Sciences (Switzerland)*, *9*(9). https://doi.org/10.3390/app9091960

Dahal, A., Chhetri, B., Sharma, K. R., & Neupane, M. (2021). Assessment of Solar Photovoltaic Potential of Building Rooftops Using Photogrammetry and GIS. *The Geographic Base*, *8*. https://doi.org/10.3126/tgbv8i01.43467

Desthieux, G., Carneiro, C., Camponovo, R., Ineichen, P., Morello, E., Boulmier, A., Abdennadher, N., Dervey, S., & Ellert, C. (2018). Solar energy potential assessment on rooftops and facades in large built environments based on lidar data, image processing, and cloud computing. Methodological background, application, and validation in Geneva (solar cadaster). *Frontiers in Built Environment*, *4*. https://doi.org/10.3389/fbuil.2018.00014

Desthieux, G., & Thebault, M. (2024). Solar governance for the transborder agglomeration of the Greater Geneva based on the solar cadaster development. *Frontiers in Built Environment*, *10*. https://doi.org/10.3389/fbuil.2024.1347056

Fish, C. S., & Calvert, K. (2016). Analysis of interactive solar energy web maps for urban energy sustainability. *Cartographic Perspectives*, *2016*(85), 5–22. https://doi.org/10.14714/CP85.1372

Formolli, M., Kleiven, T., & Lobaccaro, G. (2023). Assessing solar energy accessibility at high latitudes: A systematic review of urban spatial domains, metrics, and parameters. *Renewable and Sustainable Energy Reviews*, *177*. https://doi.org/10.1016/j.rser.2023.113231

Formolli, M., Lobaccaro, G., & Kanters, J. (2021). Solar energy in the Nordic built environment: Challenges, opportunities and barriers. *Energies*, *14*(24). https://doi.org/10.3390/en14248410

Jurasz, J. K., Dąbek, P. B., & Campana, P. E. (2020). Can a city reach energy self-sufficiency by means of rooftop photovoltaics? Case study from Poland. *Journal of Cleaner Production*, *245*. https://doi.org/10.1016/j.jclepro.2019.118813

Kanters, J., Wall, M., & Kjellsson, E. (2014). The solar map as a knowledge base for solar energy use. *Energy Procedia*, *48*, 1597–1606. https://doi.org/10.1016/j.egypro.2014.02.180

Kausika, B. B., & van Sark, W. G. J. H. M. (2021). Calibration and validation of ArcGIS solar radiation tool for photovoltaic potential determination in the Netherlands. *Energies*, *14*(7). https://doi.org/10.3390/en14071865

Kong, G., & Fan, H. (2024). Generating 3D Roof Models from ALS Point Clouds using Roof Line Topologies. Recent Advances in 3D Geoinformation Science. In Springer Cham (Ed.), *Proceedings of the 18th 3D GeoInfo Conference*.

Lobaccaro, G., Lisowska, M. M., Saretta, E., Bonomo, P., & Frontini, F. (2019). A methodological analysis approach to assess solar energy potential at the neighborhood scale. *Energies*, *12*(18). https://doi.org/10.3390/en12183554

Manni, M., Formolli, M., Boccalatte, A., Croce, S., Desthieux, G., Hachem-Vermette, C., Kanters, J., Ménézo, C., Snow, M., Thebault, M., Wall, M., & Lobaccaro, G. (2023). Ten questions concerning planning and design strategies for solar neighborhoods. *Building and Environment*, *246*. https://doi.org/10.1016/j.buildenv.2023.110946

Saretta, E., Bonomo, P., & Frontini, F. (2020). A calculation method for the BIPV potential of Swiss façades at LOD2.5 in urban areas: A case from Ticino region. *Solar Energy*, *195*, 150–165. https://doi.org/10.1016/j.solener.2019.11.062

Steadman, P., Evans, S., Liddiard, R., Godoy-Shimizu, D., Ruyssevelt, P., & Humphrey, D. (2020). Building stock energy modelling in the UK: the 3DStock method and the London Building Stock Model. *Buildings and Cities*, *1*(1), 100–119. https://doi.org/10.5334/bc.52

Stendardo, N., Desthieux, G., Abdennadher, N., & Gallinelli, P. (2020). GPU-enabled shadow casting for solar potential estimation in large urban areas. Application to the solar cadaster of Greater Geneva. *Applied Sciences (Switzerland)*, *10*(15). https://doi.org/10.3390/APP10155361

Xue, Y., Lindkvist, C. M., & Temeljotov-Salaj, A. (2021). Barriers and potential solutions to the diffusion of solar photovoltaics from the public-private-people partnership perspective – Case study of Norway. *Renewable and Sustainable Energy Reviews*, *137*. https://doi.org/10.1016/j.rser.2020.110636

Zhang, C., & Fan, H. (2022). An Improved Multi-Task Pointwise Network for Segmentation of Building Roofs in Airborne Laser Scanning Point Clouds. *Photogrammetric Record*, *37*(179), 260–284. https://doi.org/10.1111/phor.12420